Journal of Hazardous Materials 163 (2009) 418–426

Contents lists available at ScienceDirect

Journal of Hazardous Materials

journal homepage: www.elsevier.com/locate/jhazmat

Immobilization of 2,2′-dipyridyl onto bentonite and its adsorption behavior of copper(II) ions

Bilge Erdem, Adnan Özcan, Özer Gök, A. Safa Özcan*

Department of Chemistry, Faculty of Science, Anadolu University, Yunusemre Campus, 26470 Eskişehir, Turkey

ARTICLE INFO

Article history:
Received 9 March 2007
Received in revised form 30 June 2008
Accepted 30 June 2008
Available online 5 July 2008

Keywords:
Bentonite
Adsorption
2,2′-Dipyridyl
Copper
Immobilization

ABSTRACT

In this study, the immobilization of 2,2′-dipyridyl onto bentonite was firstly carried out and it was then used for the adsorption of copper(II) ions from aqueous solutions. The variation of the parameters of pH, contact time, initial copper(II) concentration and temperature were investigated in the adsorption experiments. The XRD, FTIR, elemental and thermal analyses were performed to observe the immobilization of 2,2′-dipyridyl onto natural bentonite. The adsorption data obtained were well described by the Langmuir adsorption isotherm model at all studied temperatures. The results indicated that the maximum adsorption capacity was 54.07 mg g^{-1} from the Langmuir isotherm model at 50 °C. The thermodynamic parameters indicated that the adsorption process is spontaneous, endothermic and chemical in nature. The kinetic parameters of the adsorption were calculated from the experimental data. According to these parameters, the best-fit was obtained by the pseudo-second-order kinetic model. The results showed that 2,2′-dipyridyl-immobilized bentonite can be used as the effective adsorbent for the removal of heavy metal contaminants.

1. Introduction

The removal of heavy metal ions from polluted sources has received a big deal in recent years for global of the underlying detriment of heavy metals in the environment. In addition to, they have been widely recognized that heavy metal ions in aqueous solutions create many of problems for humans, animals and plants. Although copper is essential to human life and health, it is potentially toxic at higher concentration levels. Copper is extensively discharged from the electrical industry, alloys and metal surface finishing, pulp and paper mills, fertilizer plants, petroleum refineries, and it is found as contaminant in food including shellfish, liver, mushroom, nuts and chocolate [1–6].

Human intake of large doses of copper ions leads to severe mucosal irritation and corrosion, hepatic and renal damage, central nervous system irritation, chronic disorders, cramps in the calves, to cause high fever, gastrointestinal catarrh, liver and kidney damage, and anemia [7,8]. In order to minimize the adverse effects of these kinds of heavy metals, authorities and environmental agencies all over the world enforced stringent levels for the maximum allowable limits of heavy metals discharge into the rivers, lakes and landscapes. A major effort is underway to keep copper(II) ions concentration in drinking water below the World Health Organization (WHO) maximum permissible limits of 1.00 mg dm^{-3}. Conventional treatment methods have significant disadvantages such as incomplete metal removal, high reagent consumption, generation of toxic sludge and ineffectiveness for the low metal concentrations less than 100 mg dm^{-3}, therefore their concentrations must be reduced to acceptable levels before discharging them into the environment [1,2,4].

Adsorption has proved to be one of the respective methods, which is a simple, selective and economical process for the removal of heavy metal ions from aqueous solutions. Natural adsorbents such as clay materials including montmorillonite, smectite, bentonite, sepiolite and zeolite can be used as an adsorbent for the removal of heavy metals from aqueous solutions since they are low-cost, effective, abundant and easily available. Bentonite is known as a clay material consisting essentially of smectite mineral of the montmorillonite group. It is used in many of industrial areas such as an emulsifier agent for asphaltic and resinous substances, as an adhesive agent in horticultural sprays and insecticides, in concrete mixtures, as a plasticizer in ceramic bodies as a bleaching in vegetable oils and drilling mud [9]. The inner layer of bentonite is composed of an octahedral sheet situated between two SiO_4 tetrahedral sheets. Substitutions within the lattice structure of Al^{3+} for Si^{4+} in the tetrahedral sheet and Mg^{2+} for Al^{3+} in the octahedral sheet result in unbalanced charges in the structural

* Corresponding author. Tel.: +90 222 3350580/4781; fax: +90 222 3204910.
E-mail addresses: bilgee@anadolu.edu.tr (B. Erdem), aozcan@anadolu.edu.tr (A. Özcan), ogok1@anadolu.edu.tr (Ö. Gök), asozcan@anadolu.edu.tr (A.S. Özcan).

0304-3894/$ – see front matter © 2008 Elsevier B.V. All rights reserved.
doi:10.1016/j.jhazmat.2008.06.112

units of bentonite surface. The charge imbalance is compensated by exchangeable cations including H^+, Na^+, or Ca^{2+} on the layer surfaces [10,11].

The surface properties of natural bentonite can be greatly changed with a complexation reagent by simple ion-exchange reactions. In this study, 2,2′-dipyridyl was used as a complexation agent. It occupied the exchangeable sites of bentonite. In the first time, 2,2′-dipyridyl-immobilized bentonite (DP-bentonite) was used in this study as an adsorbent for the removal of copper(II) ions to obtain information about the adsorption isotherms, thermodynamics and kinetics.

2. Materials and methods

2.1. Materials and immobilization

A stock solution of copper(II) ions was prepared by dissolving known amount of $CuSO_4{\cdot}5H_2O$ in deionized water and the stock solution was then diluted to the various concentrations between 92.5 and 200 mg dm^{-3} and the pH of the solutions was adjusted to desired values with 0.1 M HCl or 0.1 M NaOH. Fresh dilutions were used for each experiment. All the chemicals used were in analytical grade. The adsorbent was prepared by using natural bentonite, which was provided from Çanakkale, Turkey. It was crushed, ground, sieved through a 63-μm size sieve and samples collected from under the sieve and dried in an oven at 110 °C for 2 h before use.

Bentonite (30 g) was suspended in 0.8 dm^3 of deionized water and its pH was adjusted to 4.77 with acetic acid and DP-bentonite was prepared by adding 2,2′-dipyridyl at equally the cation-exchange capacity (CEC) of the bentonite. The mixture was stirred for 48 h for the immobilization of 2,2′-dipyridyl onto bentonite. When the treatment method was accomplished, the solid phase, which contains 2,2′-dipyridyl-immobilized bentonite, was separated by filtration and then washed with deionized water. It was dried, crushed, ground, sieved through a 63-μm size sieve and samples collected from under the sieve and dried in an oven at 70 °C for 24 h prior to use.

2.2. Characterization

Natural bentonite was characterized with respect to its CEC by the methylene blue method [12] and it was found as 980 mmol kg^{-1}. The BET surface areas of natural- and DP-bentonite were determined from N_2 adsorption isotherm with a surface area analyzer (Quantachrome Instruments, Nova 2200e) and the results were 67.49 and 49.66 $m^2\ g^{-1}$, respectively.

The chemical analysis of natural bentonite was conducted using an energy dispersive X-ray spectrometer (EDX-LINK ISIS 300) attached to a scanning electron microscope (SEM-Cam Scan S4). The crystalline phases present in bentonite were determined via X-ray diffractometry (XRD-Rigaku Rint 2000) using Cu Kα radiation.

Fourier Transform Infrared spectra of natural-, DP-bentonite and copper(II) loaded DP-bentonite prepared as KBr discs were recorded in a PerkinElmer Spectrum 100 Model Infrared Spectrophotometer to observe the immobilization of 2,2′-dipyridyl.

The elemental analysis (Vario EL III Elemental Analyzer, Hanau, Germany) of DP-bentonite was carried out to determine C/N ratio in DP-bentonite. Thermal analysis (Setaram) was performed to observe the immobilization of 2,2′-dipyridyl onto bentonite. The analyses for natural bentonite, 2,2′-dipyridyl and DP-bentonite were carried out in the temperature range 25–1000 °C, 25–500 °C, 25–1000 °C, respectively at a heating rate of 10 °C min^{-1}.

Zeta potential measurements of natural bentonite, DP-bentonite and DP-bentonite in the presence of copper(II) ions was determined by using a ZEN 3600 Model Zetasizer Nano-ZS connected with MPT-2 multipurpose automatic titrator (Malvern Inst. Ltd., UK). The optical device contains a 5-mW He–Ne (638 nm) laser. The sample of 0.1 g of suspensions of natural bentonite, DP-bentonite and DP-bentonite (in 50 mL of copper(II) ions solution) were sonicated for 10 min. The suspension was then kept still for 5 min to let larger particles settle. About 10 mL of clear supernatant was placed into the vial, which was connected with automatic titrator. The desired pH of the solution was kept constant during conditioning by introducing appropriate amounts of HCl or NaOH.

2.3. Adsorption studies

Adsorption experiments were firstly conducted with adsorbent in an Erlenmeyer on a magnetic stirrer to determine the optimum pH where the maximum adsorption was accomplished for copper(II) ions. The solution pH ranging from 1.5 to 5.7 was carefully adjusted the by adding a small amount of HCl or NaOH solution and measured using a pH meter (Fisher Accumet AB15), while 50 mL of 100 mg dm^{-3} copper(II) ions solutions contained in 100 mL Erlenmeyer flasks closed with stoppers were stirred using a magnetic stirrer.

The optimum pH was then determined as 5.7 and used throughout all adsorption experiments. Copper(II) ion concentrations ranging from 92.5 to 200 mg dm^{-3} were prepared and used to evaluate the adsorption isotherm data on the adsorption process. The adsorption of copper(II) ions onto DP-bentonite was carried out at constant temperatures of 20, 30, 40 and 50 °C for the adsorption isotherms. Once the optimum pH had been attained, the experiments carried out at this pH value for the increasing periods of time (10–180 min) and temperatures of 20, 30, 40 and 50 °C, until no more copper(II) ions was removed from the aqueous phase and the equilibrium had been achieved. When the adsorption procedure completed such time, the solutions were filtered and the equilibrium concentrations were then analyzed for residual copper(II) ion concentrations by using an atomic absorption spectrophotometer (PerkinElmer) with an air–acetylene flame. Deuterium background correction was used. The instrument calibration was periodically checked by using standard metal solutions for every 15 reading. The amount of copper(II) ions adsorbed onto DP-immobilized bentonite was determined by the difference between the initial and the remaining concentrations of copper(II) ions solution.

3. Results and discussion

3.1. Chemical composition of bentonite

The chemical composition of natural bentonite, which is obtained by using EDX analysis, is given as following (%): SiO_2: 70.75, Al_2O_3: 16.18, K_2O: 2.12, CaO: 1.62, MgO: 1.25, Fe_2O_3: 0.70, TiO_2: 0.18, Na_2O: 0.11 and loss of ignition: 6.63. This result indicates the presence of silica and alumina as major constituents along with traces of sodium, potassium, iron, magnesium, calcium, and titanium oxides in the form of impurities. XRD results combined with EDX analysis show that most of the silicon is in the form of bentonite. XRD also indicates the presence of free quartz in bentonite. It is, thus, expected that the adsorbate species will be removed mainly by SiO_2 and Al_2O_3.

The XRD patterns of natural bentonite and DP-bentonite were recorded (Fig. 1) and their basal spaces were observed at 14.87 and 14.72 Å, respectively. The expansion in the basal spacing of the

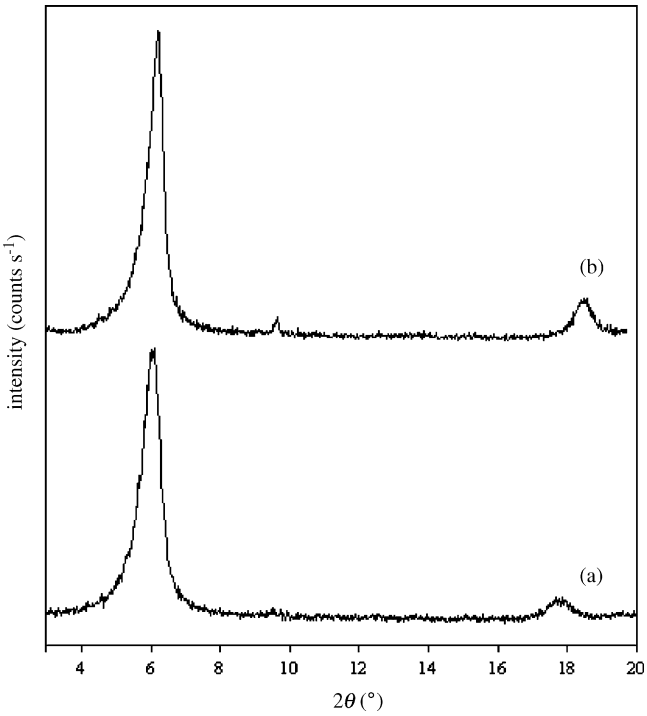

Fig. 1. XRD patterns of (a) natural bentonite and (b) DP-bentonite.

natural bentonite can be calculated as $\Delta d = d - 14.87$ Å, where d is the basal spacing of the DP-immobilized bentonite and 14.72 Å is the thickness of a clay layer [13]. Δd is found to be −0.15 Å. This result suggests that the expansion in the basal spacing of natural bentonite with complexation reagent was not observed and 2,2′-dipyridyl attach to the edges of bentonite.

3.2. FTIR analysis

The FTIR spectra of natural bentonite, DP-bentonite and copper(II)-loaded DP-bentonite (Fig. 2) were performed in the range of 4000–400 cm^{-1} and compared with each other to obtain information on the immobilization of the 2,2′-dipyridyl onto bentonite and the nature of the possible DP-bentonite–metal ions interactions.

A group of absorption peaks observes between 3433 and 3623 cm^{-1}, which is due to H–O–H stretching vibration bands of water molecules weakly hydrogen bonded to the Si–O surface in the natural bentonite (Fig. 2(a)) and DP-bentonite (Fig. 2(b)) and their bending vibrations at 915 and 845 cm^{-1}. The above stretching band intensities of DP-bentonite were rather lower than that of natural bentonite. The stretching vibration of aromatic C–H groups is observed at 3101 cm^{-1}. This band is the first evidence for the immobilization of 2,2′-dipyridyl onto edges of bentonite. The band at around 1635 cm^{-1} also corresponds to the –OH deformation of water to observe natural bentonite and DP-bentonite. The C–C and C–N ring stretching (skeletal) vibrations in the DP-bentonite (Fig. 2(b)) were observed at 1587, 1531, 1472 and 1459 cm^{-1} (four bands) and the γ_{C-H} bending and β-ring vibrations obtained at 726 and 765 cm^{-1}, respectively [14], but these bands were not observed in the natural bentonite. This may be the second acceptable evidence for the immobilization of 2,2′-dipyridyl onto natural bentonite.

The C–C and C–N ring stretching (skeletal) bands in the copper(II)-loaded DP-bentonite (Fig. 2(c)) shifts 1577, 1502, 1477 and 1453 cm^{-1} and their γ_{C-H} bending and β-ring vibrations moves at 729 and 750 cm^{-1}, respectively to compare with the related DP-bentonite bands. This behavior reflects the interaction between DP-bentonite and copper(II) ions.

The Si–O coordination bands at 1087 and 1039 cm^{-1} are observed as a result of the Si–O vibrations. The deep band at around 1039 cm^{-1} represents the stretching of Si–O in the Si–O–Si groups of the tetrahedral sheet. The bands at 523 and 467 cm^{-1} are due to Si–O–Al (octahedral) and Si–O–Si bending vibrations respectively, for each sample. The Si–O stretching vibration at around 1039 cm^{-1} shifts 1047 cm^{-1} after the copper(II) ions loaded. It confirms that there is an interaction between DP-bentonite and copper(II) ions.

3.3. Elemental and thermal analysis

The ratio of C/N for DP-bentonite from elemental analysis results is 4.335 and the calculated value of C/N ratio is 4.287. The percentage of 2,2′-dipyridyl immobilization onto bentonite is 8.918. These results confirm that the 2,2′-dipyridyl molecules immobilized onto bentonite and they are also consistent with above FTIR analysis results.

The differential thermogravimetric (DTG) analysis curves of the natural bentonite, 2,2′-dipyridyl and DP-bentonite were indicated that the peak at around 260 °C was only observed in DP-immobilized bentonite and it confirms the immobilization of

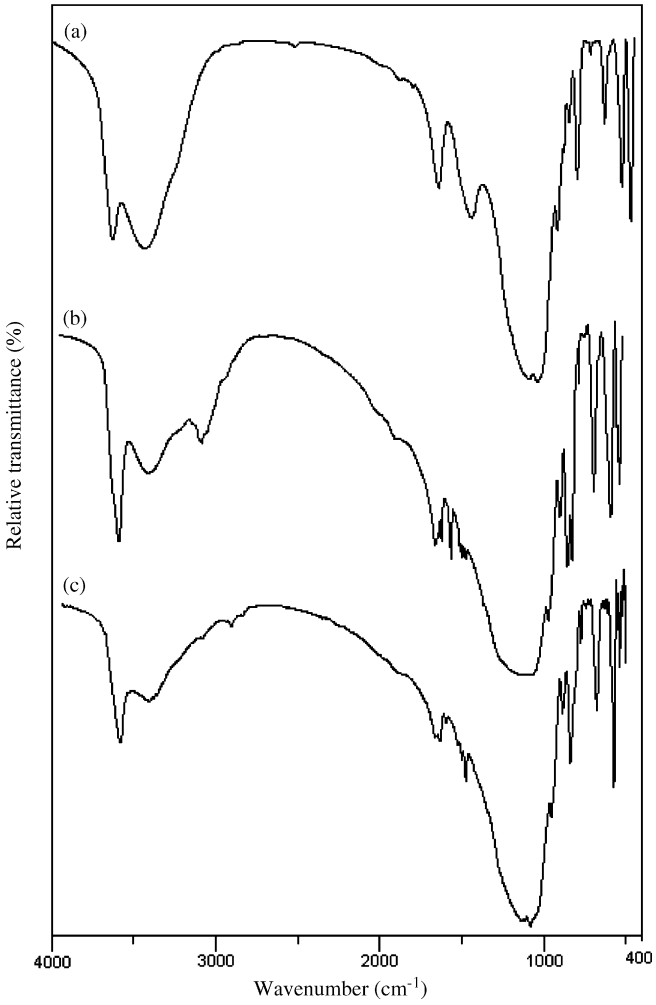

Fig. 2. FTIR spectra of (a) natural bentonite, (b) DP-bentonite and (c) copper(II) ions loaded DP-bentonite.

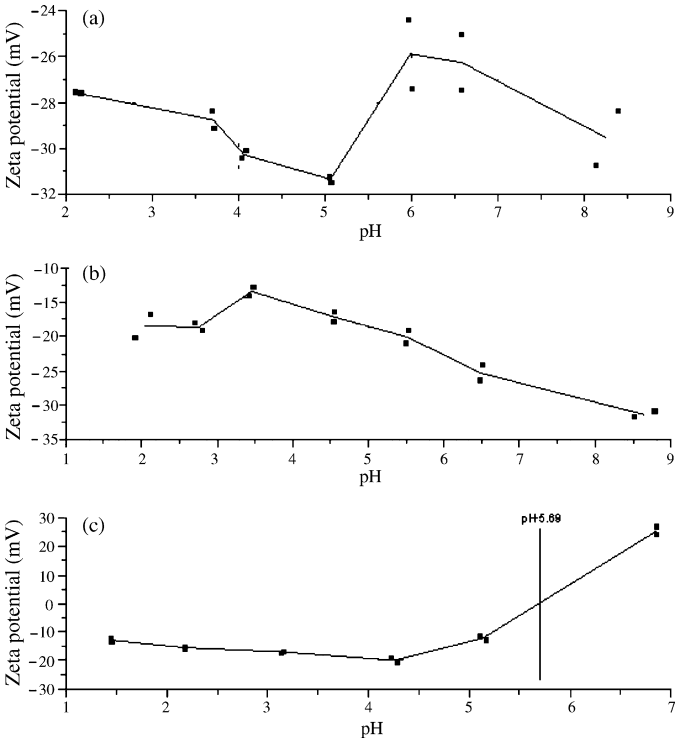

Fig. 3. The zeta potential of (a) natural bentonite, (b) DP-bentonite and (c) copper(II) ions loaded DP-bentonite solution as a function of pH.

the 2,2′-dipyridyl onto bentonite but this peak is not observed in natural bentonite.

3.4. Zeta potential measurements

The zeta potential of natural bentonite, DP-immobilized bentonite and DP-immobilized bentonite (in copper(II) ions solution) was depicted in Fig. 4, as a function of suspension pH. As shown in Fig. 3(a) and (b), natural bentonite and DP-bentonite have no point of zero charge (pH_{pzc}) and exhibit negative zeta potential values at all studied pH values. This result agrees with those obtained from electrokinetic measurements of clay minerals [15–18].

The zeta potential is important in the case of DP-bentonite in copper(II) ions solution and dependent on pH (Fig. 3(c)). The point of zero charge, where the colloidal system is least stable [19], was measured as 5.69 for DP-bentonite in copper(II) ions solution. After this point (pH > 5.69), the surface charge becomes increasingly positive, but the natural bentonite and DP-immobilized bentonite (the absence of copper(II) ions) have a negative charge (Fig. 3(a) and (b)), while copper(II) ions tends to form a cationic species and consequently, has a positive surface charge (Fig. 3(c)), thus the electrostatic interactions between the surface and copper(II) ions complexes are considerable. Therefore, changes to the sign of the zeta potential of DP-bentonite in the presence of copper(II) ions can be directly related to the specific adsorption of cationic copper(II) ions species [20].

3.5. Effect of pH

The pH of aqueous solution has been known as the most important variable governing heavy metal adsorption onto adsorbent. This is partly because hydrogen ions themselves are strongly competing with adsorbates. Fig. 4 indicates the effect of pH on the removal of copper(II) ions onto natural bentonite and DP-bentonite from aqueous solutions. It can be seen from Fig. 4 that the adsorption capacity are almost same up to pH 4.0. After pH 4.0, uptakes increase sharply up to pH 5.0 and then it was stable up to pH 5.7 since more metal binding sites could be exposed and carried negative charges, with subsequent attraction of metal ions with positive charge and adsorption onto the adsorbent surface. Experiments were not carried out after the pH values of up to 5.7 due to the fact that metal precipitation appeared at higher pH values and interfered with the accumulation or adsorbent deterioration [21].

3.6. Adsorption isotherms

The adsorption data were analyzed to see whether the isotherm obeyed the Langmuir [22], Freundlich [23] and Dubinin–Radushkevich (D–R) [24] isotherm models. The linear forms of the Langmuir, Freundlich and Dubinin–Radushkevich (D–R) isotherm equations are represented by the following equations:

- Langmuir:

$$\frac{C_e}{q_e} = \frac{1}{q_{max}K_L} + \frac{C_e}{q_{max}} \quad (1)$$

- Freundlich:

$$\ln q_e = \ln K_F + \frac{1}{n}\ln C_e \quad (2)$$

- Dubinin–Radushkevich (D–R):

$$\ln q_e = \ln q_m - \beta\varepsilon^2 \quad (3)$$

where q_e is the equilibrium copper(II) ions concentration on the adsorbent ($mg\,g^{-1}$), C_e is the equilibrium copper(II) ions concentration in solution ($mg\,dm^{-3}$), q_{max} is the monolayer capacity of the adsorbent ($mg\,g^{-1}$) and K_L is the Langmuir constant ($dm^3\,mg^{-1}$) and related to the free energy of adsorption; K_F ($dm^3\,g^{-1}$) is Freundlich constant and n (dimensionless) is the heterogeneity factor which has a lower value for more heterogeneous surfaces; β is a constant related to the mean free energy of adsorption per mole of the adsorbate ($mol^2\,kJ^{-2}$), q_m is the theoretical saturation capacity ($mol\,g^{-1}$), and ε is the Polanyi potential, which is equal to $RT\ln(1+(1/C_e))$, where R ($J\,mol^{-1}\,K^{-1}$) is the gas constant, and T (K) is the absolute temperature. The plots of C_e/q_e versus C_e (Langmuir) for the adsorption of copper(II) ions onto DP-bentonite (Fig. 5) give a straight line of slope $1/q_{max}$

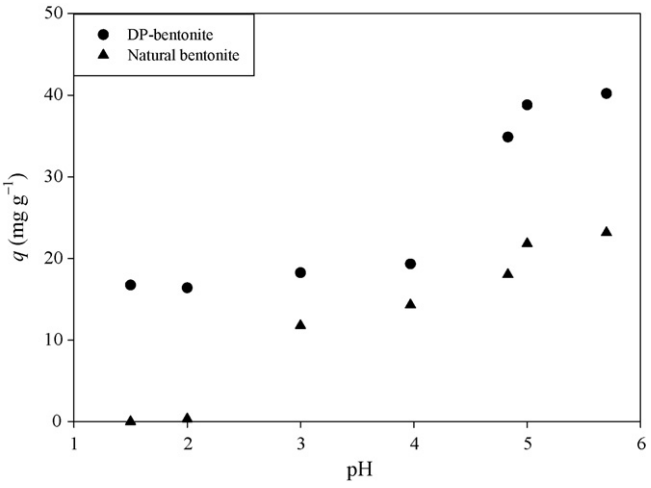

Fig. 4. Effect of pH for the adsorption of copper(II) ions onto natural bentonite and DP-bentonite at 20 °C.

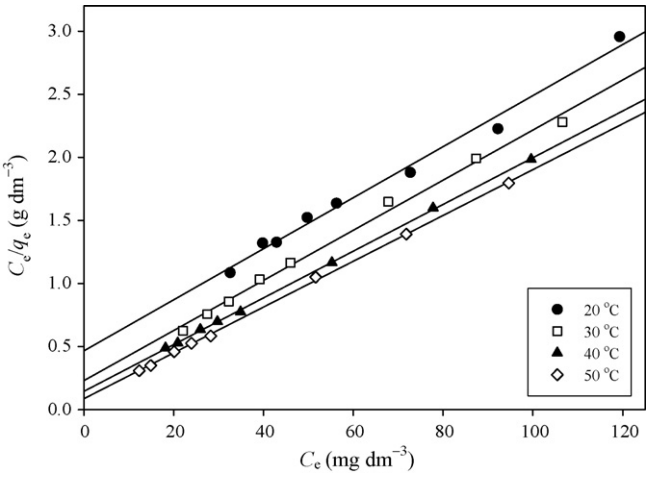

Fig. 5. Langmuir plots for the adsorption of copper(II) ions onto DP-bentonite at various temperatures.

and intercept $1/q_{max}\,K_L$, by plotting $\ln C_e$ versus $\ln q_e$ (figure not shown) (Freundlich) to generate the intercept value of K_F and the slope value n and by plotting $\ln q_e$ versus ε^2 (figure not shown) (Dubinin–Radushkevich (D–R)) it is possible to obtain the value of q_m from the intercept, and the value of β from the slope.

The Langmuir, Freundlich and D–R parameters for the adsorption of copper(II) ions onto DP-bentonite are being listed in Table 1. It is evident from these data that the adsorption of copper(II) ions onto DP-bentonite is fitted well the Langmuir isotherm model than that of the Freundlich and D–R isotherm models, as indicated by the r^2 values in Table 1.

The effect of isotherm shape has been studied [25] with the goal of predicting whether an adsorption system is favorable or unfavorable. The essential feature of the Langmuir isotherm can be expressed by means of 'R_L', a dimensionless constant referred to as the separation factor, or equilibrium parameter. R_L is calculated by using the following equation:

$$R_L = \frac{1}{1 + K_L C_0} \tag{4}$$

where C_0 is the copper(II) ions concentration (mg dm^{-3}). The values of R_L are incorporated in Table 1. If R_L values lie between 0 and 1, adsorption process is considered to be favorable [25,26]. The R_L values in this study ranged from 5.48×10^{-2} to 0.103, indicating that the adsorption process is favorable.

The maximum adsorption capacity of DP-bentonite obtained for copper(II) ions in this study was found to be comparable and higher than those of many corresponding clay related adsorbents reported in the literature [27–40] (Table 2).

One of the Freundlich constants K_F indicates the adsorption capacity of the adsorbent. The other Freundlich constants n is a measure of the deviation from linearity of the adsorption. The numerical values of n at equilibrium lie between 3.584 and 7.859 are greater than unity, indicating that copper(II) ions is favorably adsorbed by DP-bentonite at all the studied temperatures.

Table 2
Adsorption results of copper(II) ions from the literature by various clay-based adsorbents

Adsorbent	Adsorption capacity (mg g^{-1})
Montmorillonite [27]	28.80
TBA-montmorillonite [27]	27.30
TBA-kaolinite [27]	3.20
Manganese oxide coated zeolite [28]	6.34
Natural bentonite [29]	44.84
Kaolin [30]	4.47
Diatomite [30]	5.54
Vermiculite [31]	20.61
Clay-Bulgarian [32]	3.11
Palygorskite clay [33]	30.70
Spent activated clay [34]	13.20
Clinoptilolite [35]	3.80
Natural zeolite [36]	8.96
Kaolinite [37]	10.79
Commercial bentonite [38]	23.43
CBDA-hectorite [39]	40.64
Ca-bentonite [40]	7.72
Na-bentonite [40]	30.00
2,2′-Dipyridyl-immobilized bentonite (in this study)	54.07

The constant β gives an idea of the mean free energy E (kJ mol^{-1}) of adsorption per mol of the adsorbate when it is transferred to the surface of the solid from infinity in the solution, and can be calculated using the relationship [41]:

$$E = \frac{1}{(2\beta)^{1/2}} \tag{5}$$

This parameter gives information about the type of adsorption mechanism as chemical ion-exchange or physical adsorption. A value of E between 8 and 16 kJ mol^{-1} corresponds to a chemical ion-exchange process whereas values <8 kJ mol^{-1} represent a physical type of process [42]. The numerical value of E was found to be >8 kJ mol^{-1} for all studied temperatures, indicating that the adsorption may occur via a chemical ion-exchange process.

3.7. Thermodynamic parameters

In any adsorption procedure, both energy and entropy considerations should be taken into account in order to determine what process will take place spontaneously. Values of thermodynamic parameters are the actual indicators for practical application of a process. The amount of copper(II) ions adsorbed at equilibrium at different temperatures is 20, 30, 40 and 50 °C, have been examined to obtain the thermodynamic parameters for the adsorption system.

Because K_L is the Langmuir constant and its dependence with temperature that can be used to predict thermodynamic parameters, such as changes in the Gibbs free energy (ΔG°), enthalpy (ΔH°) and entropy (ΔS°) associated to the adsorption process and were determined by using following equations:

$$\Delta G^\circ = -RT \ln K_L \tag{6}$$

Table 1
Isotherm constants for the adsorption of copper(II) ions onto DP-bentonite at various temperatures

(°C)	Langmuir				Freundlich			Dubinin–Radushkevich (D–R)			
	q_{max} (mg g^{-1})	K_L (dm^3 mg^{-1})	R_L	r_L^2	n	K_F (dm^3 g^{-1})	r_F^2	q_m (mg g^{-1})	β (mol^2 kJ^{-2})	r_{D-R}^2	E (kJ mol^{-1})
20	49.44	4.33×10^{-2}	0.103	0.989	3.584	11.20	0.924	93.94	3.40×10^{-3}	0.929	12.12
30	50.33	8.62×10^{-2}	5.48×10^{-2}	0.995	5.929	20.72	0.973	73.24	1.85×10^{-3}	0.966	16.45
40	54.01	0.127	3.79×10^{-2}	0.999	6.005	23.85	0.940	82.54	1.69×10^{-3}	0.952	17.19
50	54.07	0.208	2.33×10^{-2}	0.999	7.859	30.02	0.931	76.16	1.17×10^{-3}	0.947	20.71

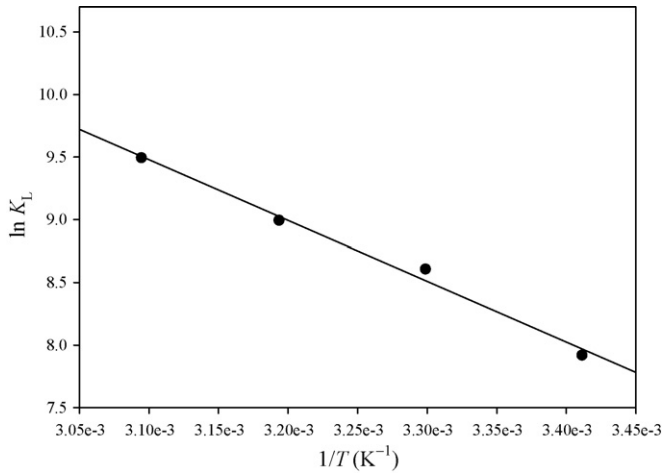

Fig. 6. Plot of $\ln K_L$ vs. $1/T$ for the predicting of thermodynamic parameters for the adsorption of copper(II) ions onto DP-bentonite.

$$\ln K_L = -\frac{\Delta G^\circ}{RT} = -\frac{\Delta H^\circ}{RT} + \frac{\Delta S^\circ}{R} \quad (7)$$

The plot of $\ln K_L$ as a function of $1/T$ (Fig. 6) yields a straight line from which ΔH° and ΔS° were calculated from the slope and intercept, respectively.

The overall free energy changes during the adsorption process were $-19.30\,kJ\,mol^{-1}$ at 20 °C, $-21.70\,kJ\,mol^{-1}$ at 30 °C, $-23.42\,kJ\,mol^{-1}$ at 40 °C and $-25.51\,kJ\,mol^{-1}$ at 50 °C, which were all negative, corresponding to a spontaneous process of copper(II) ions adsorption.

The high positive value of the enthalpy change ($+40.32\,kJ\,mol^{-1}$) indicates that the adsorption is chemical in nature involving strong forces of attraction and is also endothermic [43]. The positive entropy change (ΔS°) value ($+203.80\,J\,mol^{-1}\,K^{-1}$) corresponds to an increase in the degree of freedom of the adsorbed species.

3.8. Adsorption kinetics

The influence of contact time on the adsorption of copper(II) ions onto DP-bentonite (Fig. 7) was investigated at various temperatures, i.e. 20, 30, 40 and 50 °C. It is easily seen that the amount of adsorption increased with the increasing of contact time. Maximum adsorption capacity was observed after 50 min, beyond which

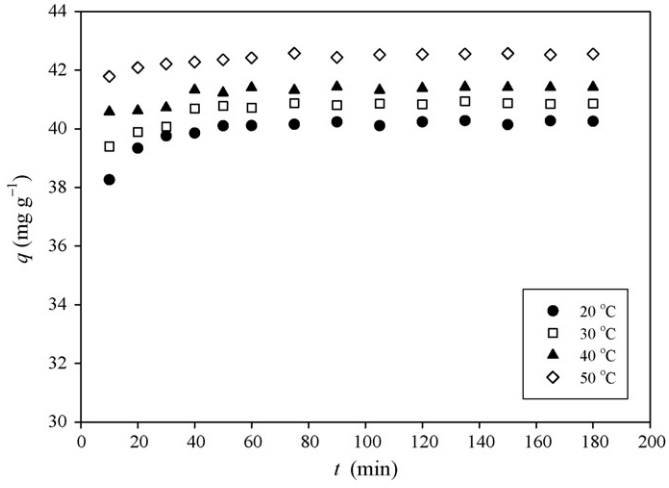

Fig. 7. Effect of contact time for the adsorption of copper(II) ions onto DP-bentonite at various temperatures.

there was almost no further increase in the adsorption. This was therefore fixed as the equilibrium contact time.

The equilibrium adsorption capacity of copper(II) ions onto DP-bentonite for the pseudo-second-order kinetic model was found to increase with increasing temperature from 20 to 50 °C (Fig. 7), indicating that copper(II) ions adsorption on the adsorbent was favored at higher temperatures. This effect suggests that an explanation of the adsorption mechanism associated with the removal of copper(II) ions onto DP-bentonite involves a temperature dependent process.

Four kinetic model equations, i.e. the Lagergren-first-order, pseudo-second-order, Elovich and the intraparticle diffusion, were considered to interpret the experimental data.

The Lagergren-first-order rate expression [44] is given as

$$\ln(q_1 - q_t) = \ln q_1 - k_1 t \quad (8)$$

The pseudo-second-order kinetic model equation [45] is given as

$$\frac{t}{q_t} = \frac{1}{k_2 q_2^2} + \frac{1}{q_2} t \quad (9)$$

The Elovich equation is generally expressed as follows [46]:

$$\frac{dq_t}{dt} = \alpha \exp(-\beta q_t) \quad (10)$$

To simplify the Elovich equation, Chien and Clayton [47] assumed $\alpha\beta t \gg 1$ and by applying the boundary conditions $q_t = 0$ at $t = 0$ and $q_t = q_t$ at $t = t$ Eq. (10) becomes [48]:

$$q_t = \frac{1}{\beta} \ln(\alpha\beta) + \frac{1}{\beta} \ln t \quad (11)$$

The intraparticle diffusion equation [49] can be written by using the following equation:

$$q_t = k_p t^{1/2} + C \quad (12)$$

where q_1 and q_t are the amounts of copper(II) ions adsorbed on the adsorbent at equilibrium and at various times t (mg g^{-1}) and k_1 is the rate constant of the Lagergren-first-order model for the adsorption process (min^{-1}); q_2 is the maximum adsorption capacity (mg g^{-1}) for the pseudo-second-order adsorption and k_2 is the rate constant of the pseudo-second-order model for the adsorption process (g mg^{-1} min^{-1}); α is the initial adsorption rate (mg g^{-1} min^{-1}) and β is the desorption constant (g mg^{-1}) for Elovich equation during any one experiment; C is the intercept and k_p is the intraparticle diffusion rate constant (mg g^{-1} min$^{-1/2}$). The straight-line plots of $\ln(q_1 - q_t)$ versus t for the Lagergren-first-order model (figure not shown), t/q_t against t for the pseudo-second-order model (Fig. 8) and the plots of q_t versus $\ln(t)$ (figure not shown) for the Elovich model for the adsorption of copper(II) ions onto DP-bentonite have been drawn to obtain the rate parameters.

The kinetic parameters of copper(II) ions onto DP-bentonite under different conditions were calculated from these plots and are given in Table 3. It can be easily seen from Table 3, the correlation coefficients (r_1^2 and r_E^2), for the Lagergren-first-order and for the Elovich kinetic models are lower than that of the pseudo-second-order kinetic model. They are probable, therefore, that these adsorption systems are not followed by the Lagergren-first-order or Elovich kinetic models, they are fitted the pseudo-second-order kinetic model. The calculated q_2 values agree with experimental q values, and also, the correlation coefficients for the pseudo-second-order kinetic plots were very high.

The pseudo-second-order rate constants increase from 4.89×10^{-2} to 9.28×10^{-2} g mg^{-1} min^{-1} with an increase in the solution temperatures from 20 to 50 °C at 100 mg dm^{-3}

Table 3
Kinetic parameters and the normalized standard deviations for the adsorption of copper(II) ions onto DP-bentonite at various temperatures

T (°C)	C_0 (mg dm^{-3})	Lagergren-first-order				Pseudo-second-order				Elovich				Intraparticle diffusion			
		k_1 (min^{-1})	q_1 (mg g^{-1})	Δq (%)	r_1^2	k_2 (g mg^{-1} min^{-1})	q_2 (mg g^{-1})	Δq (%)	r_2^2	α (mg g^{-1} min^{-1})	β (g mg^{-1})	Δq (%)	r_E^2	k_p (mg g^{-1} min$^{-1/2}$)	C (mg g^{-1})	Δq (%)	r_p^2
20	100	3.71×10^{-2}	1.869	–	0.737	4.89×10^{-2}	40.38	0.796	0.999	7.36×10^{28}	1.784	1.793	0.780	0.449	37.08	1.338	0.906
	125	3.12×10^{-2}	1.771	–	0.672	4.67×10^{-2}	45.93	0.952	0.999	8.87×10^{32}	1.774	1.669	0.887	0.335	43.12	1.530	0.974
	150	3.36×10^{-2}	1.983	–	0.766	4.60×10^{-2}	46.69	1.104	0.999	9.03×10^{31}	1.695	1.533	0.809	0.427	43.44	1.251	0.834
	175	4.55×10^{-2}	4.568	–	0.932	2.76×10^{-2}	47.64	1.228	0.999	1.40×10^{23}	1.231	1.690	0.893	0.370	44.07	1.754	0.867
	200	3.24×10^{-2}	3.994	–	0.762	1.99×10^{-2}	48.33	2.071	0.999	2.50×10^{21}	1.132	2.301	0.876	0.240	45.09	2.192	0.927
30	100	3.14×10^{-2}	1.501	–	0.803	6.09×10^{-2}	40.99	0.633	0.999	5.69×10^{33}	2.035	0.886	0.821	0.367	38.22	0.843	0.963
40	100	2.47×10^{-2}	0.864	–	0.642	7.62×10^{-2}	41.50	0.584	0.999	3.37×10^{52}	3.064	0.670	0.786	0.201	39.83	0.948	0.763
50	100	1.96×10^{-2}	0.799	–	0.763	9.28×10^{-2}	42.62	0.559	0.999	5.49×10^{70}	3.974	0.861	0.907	0.140	41.41	0.752	0.945

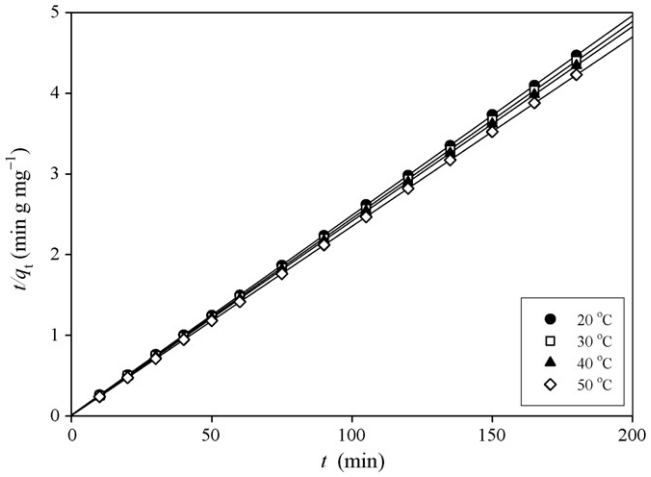

Fig. 8. Pseudo-second-order kinetic plots for the adsorption of copper(II) ions onto DP-bentonite at various temperatures.

(Table 3), indicating that the adsorption of copper(II) ions onto DP-bentonite is the rate-controlled.

The first-order, pseudo-second-order and Elovich models cannot identify the diffusion mechanism and the kinetic results were then subjected to analyze by the intraparticle diffusion model and it may be the rate-controlling step. If this does occur, then the plot of uptake, q_t, versus square root of time, $t^{1/2}$, should be linear and if it passes through the origin then the intraparticle diffusion will be the sole rate-limiting process [50–53]. In this study, it was found that the plots of q_t versus $t^{1/2}$ exhibited an initial linear portion followed by a plateau which occurred after 50 min for DP-bentonite (figure not shown). The initial curved portion of the plots seems to be due to boundary layer adsorption and the linear portion to intraparticle diffusion, with the plateau corresponding to equilibrium [53]. However, neither plot passed through the origin. This indicates that although intraparticle diffusion was involved in the adsorption process, it was not the rate-controlling step. Values of the intraparticle diffusion constant, k_p, were obtained from the slopes of the linear portions of the plots and are listed in Table 3. The correlation coefficients for the intraparticle diffusion model (r_p^2) were between 0.763 and 0.974. These values indicate that the adsorption of copper(II) ions onto DP-bentonite may be followed by the intraparticle diffusion up to 50 min.

The validity of used kinetic models in this study can be quantitatively checked by using a normalized standard deviation Δq (%) calculated by using the following equation [54]:

$$\Delta q(\%) = \sqrt{\frac{\sum [(q_{exp} - q_{cal})/q_{exp}]^2}{n-1}} 100 \quad (13)$$

where n is the number of data points and the calculated results are listed in Table 3. As it can be seen from Table 3, the values of Δq (%) for the best-fit model are less than 2.072%. It is concluded that the adsorption of copper(II) ions onto DP-bentonite can be best described by the pseudo-second-order kinetic model.

3.9. Suggested copper(II) ions adsorption mechanism with 2,2′-dipyridyl-immobilized bentonite (DP-bentonite)

The immobilization agent, 2,2′-dipyridyl, was used in this study and DP-bentonite was then examined as an adsorbent for the adsorption copper(II) ions from aqueous solution. Bentonite consists of the silanol and aluminol groups. The silanol groups may be the responsible for the immobilization of DP onto bentonite. The results indicate that DP-bentonite can easily adsorb copper(II) ions

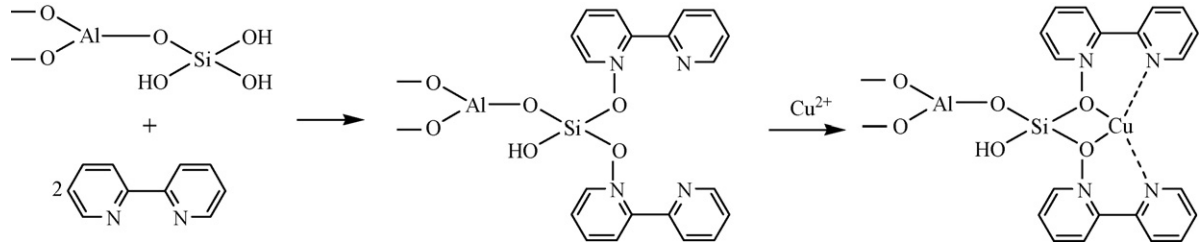

Fig. 9. The possible mechanism for the adsorption of copper(II) ions onto DP-bentonite.

a possible mechanism by using silanol –OH groups as can be seen from Fig. 9.

4. Conclusions

In this study, the equilibrium, thermodynamics and kinetic parameters of copper(II) ions onto DP-bentonite in aqueous solutions was investigated. It may be concluded that DP-bentonite acts a respective adsorbent for the removal of copper(II) ions in aqueous solutions due to its high adsorption capacity. The maximum adsorption capacity was found to be 54.07 mg g^{-1} at pH 5.7 and 50 °C.

The functional groups of natural bentonite, DP-bentonite and copper(II)-loaded DP-bentonite were determined by using FTIR spectrophotometer. The isoelectric point (pH_{pzc}) of DP-bentonite in copper(II) ions solution was determined as 5.69.

The straight lines obtained for the Langmuir, Freundlich and Dubinin–Radushkevich (D–R) models obey to fit to the experimental equilibrium data, but the Langmuir isotherm model gives better fittings than the Freundlich and D–R isotherm models. The thermodynamic parameters obtained from Langmuir constant (K_L) indicate a chemical, feasible, spontaneous and endothermic adsorption.

The pseudo-second-order kinetic model agrees very well with the dynamic behavior for the adsorption of copper(II) ions onto DP-bentonite at various temperatures. The experimental data have also been applied to predict the rate constants of adsorption and adsorption capacities. However, the evidence is provided that the adsorption of copper(II) ions onto DP-bentonite is a complex process, so it cannot be sufficiently described by a single kinetic model throughout the whole process. For instance, intraparticle diffusion (up to 50 min) played a significant role, however, it was not the main rate determining step during the adsorption.

The results indicate that DP-bentonite can easily adsorb copper(II) ions by a possible mechanism. The silanol –OH groups can be played a main role in the mechanism.

References

[1] L. Wang, H. Chua, S.N. Sin, Q. Zhou, D.M. Ren, Z.L. Li, A combined bioprocess for integrated removal of copper and organic pollutant from copper-containing municipal wastewater, J. Environ. Sci. Health A: Toxic Hazard. Subst. Environ. Eng. 39 (1) (2004) 223–235.
[2] R. Han, J. Zhang, W. Zou, H. Xiao, J. Shi, H. Liu, Biosorption of copper(II) and lead(II) from aqueous solution by chaff in a fixed-bed column, J. Hazard. Mater. 133 (1–3) (2006) 262–268.
[3] J.C. Shen, Z. Duvnjak, Effects of temperature and pH on adsorption isotherms for cupric and cadmium ions in their single and binary solutions using corncob particles as adsorbent, Sep. Sci. Technol. 39 (13) (2004) 3023–3041.
[4] P. King, P. Srinivas, Y.P. Kumar, V.S.R.K. Prasad, Sorption of copper(II) ion from aqueous solution by *Tectona grandis* l.f. (teak leaves powder), J. Hazard. Mater. 136 (3) (2006) 560–566.
[5] N. Li, R. Bai, Copper adsorption on chitosan-cellulose hydrogel beads: behaviors and mechanisms, Sep. Purif. Technol. 42 (3) (2005) 237–247.
[6] V.K. Gupta, A. Rastogi, V.K. Saini, N. Jain, Biosorption of copper(II) from aqueous solutions by *Spirogyra* species, J. Colloid Interf. Sci. 296 (1) (2006) 59–63.
[7] M. Ajmal, R.A.K. Rao, M.A. Khan, Adsorption of copper from aqueous solution on *Brassica cumpestris* (mustard oil cake), J. Hazard. Mater. 122 (1/2) (2005) 177–183.
[8] S. Larous, A.-H. Meniai, M.B. Lehocine, Experimental study of the removal of copper from aqueous solutions by adsorption using sawdust, Desalination 185 (1–3) (2005) 483–490.
[9] G. Montes-H, Y. Geraud, Sorption kinetic of water vapour of MX80 bentonite submitted to different physical-chemical and mechanical conditions, Colloids Surf. A: Physicochem. Eng. Aspects 235 (1–3) (2004) 17–23.
[10] Y.-H. Shen, Preparation of organobentonite using non-ionic surfactants, Chemosphere 44 (5) (2001) 989–995.
[11] A.S. Özcan, A. Özcan, Adsorption of acid dyes from aqueous solutions onto acid-activated bentonite, J. Colloid Interf. Sci. 276 (1) (2004) 39–46.
[12] R.K. Taylor, Cation exchange in clays and mudrocks by methylene blue, J. Chem. Technol. Biotechnol. 35A (1985) 195–207.
[13] G. Akçay, M. Akçay, K. Yurdakoç, Removal of 2,4-dichlorophenoxyacetic acid from aqueous solutions by partially characterized organophilic sepiolite: thermodynamic and kinetic calculations, J. Colloid Interf. Sci. 281 (1) (2005) 27–32.
[14] R.M. Silverstein, F.X. Webster, Spectrometric Identification of Organic Compounds, 6th ed., John Wiley, New York, 1998.
[15] A. Delgado, F. González-Caballero, J.M. Bruque, On the zeta potential and surface charge density of montmorillonite in aqueous electrolyte solutions, J. Colloid Interf. Sci. 113 (1) (1986) 203–211.
[16] Y. Horikawa, R.S. Murray, J.P. Quirk, The effect of electrolyte concentration on the zeta potentials of homoionic montmorillonite and illite, Colloids Surf. 32 (1988) 181–195.
[17] D.J.A. Williams, K.P. Williams, Electrophoresis and zeta potential of kaolinite, J. Colloid Interf. Sci. 65 (1) (1978) 79–87.
[18] A. Chakir, J. Bessiere, K.E.L. Kacemi, B. Marouf, A comparative study of the removal of trivalent chromium from aqueous solutions by bentonite and expanded perlite, J. Hazard. Mater. 95 (1/2) (2002) 29–46.
[19] R.J. Hunter, Zeta Potential in Colloid Science: Principles and Applications, Academic Press, UK, 1988.
[20] J.S. Laskowski, Electrokinetic measurements in aqueous solutions of weak electrolyte type surfactants, J. Colloid Interf. Sci. 159 (2) (1993) 349–353.
[21] M.S. Alhakawati, C.J. Banks, Removal of copper from aqueous solution by *Ascophyllum nodosum* immobilised in hydrophilic polyurethane foam, J. Environ. Manage. 72 (4) (2004) 195–204.
[22] I. Langmuir, The adsorption of gases on plane surfaces of glass, mica and platinum, J. Am. Chem. Soc. 40 (9) (1918) 1361–1403.
[23] H.M.F. Freundlich, Über die adsorption in lösungen, Z. Phys. Chem. 57 (1906) 385–470.
[24] M.M. Dubinin, L.V. Radushkevich, Proc. Acad. Sci. U.S.S.R. Phys. Chem. Sect. 55 (1947) 331–333.
[25] K.R. Hall, L.C. Eagleton, A. Acrivos, T. Vermeulen, Pore- and solid-diffusion kinetics in fixed-bed adsorption under constant-pattern conditions, Ind. Eng. Chem. Fundam. 5 (2) (1966) 212–223.
[26] T.W. Weber, R.K. Chakravorti, Pore and solid diffusion models for fixed-bed adsorbers, J. Am. Inst. Chem. Eng. 20 (2) (1974) 228–238.
[27] K.G. Bhattacharyya, S.S. Gupta, Kaolinite, montmorillonite, and their modified derivatives as adsorbents for removal of Cu(II) from aqueous solution, Sep. Purif. Technol. 50 (3) (2006) 388–397.
[28] W. Zou, R. Han, Z. Chen, Z. Jinghua, J. Shi, Kinetic study of adsorption of Cu(II) and Pb(II) from aqueous solutions using manganese oxide coated zeolite in batch mode, Colloids Surf. A: Physicochem. Eng. Aspects 279 (1–3) (2006) 238–246.
[29] S. Veli, B. Alyüz, Adsorption of copper and zinc from aqueous solutions by using natural clay, J. Hazard. Mater. 149 (1) (2007) 226–233.
[30] M. Ulmanu, E. Marañón, Y. Fernández, L. Castrillón, I. Anger, D. Dumitriu, Removal of copper and cadmium ions from diluted aqueous solutions by low cost and waste material adsorbents, Water Air Soil Pollut. 142 (1–4) (2003) 357–373.
[31] M. Malandrino, O. Abollino, A. Giacomino, M. Aceto, E. Mentasti, Adsorption of heavy metals on vermiculite: influence of pH and organic ligands, J. Colloid Interf. Sci. 299 (2) (2006) 537–546.
[32] I. Atanassova, M. Okazaki, Adsorption–desorption characteristics of high levels of copper in soil clay fractions, Water Air Soil Pollut. 98 (3/4) (1997) 213–228.
[33] J.H. Potgieter, S.S. Potgieter-Vermaak, P.D. Kalibantonga, Heavy metals removal from solution by palygorskite clay, Miner. Eng. 19 (5) (2006) 463–470.

[34] C.-H. Weng, C.-Z. Tsai, S.-H. Chu, Y.C. Sharma, Adsorption characteristics of copper(II) onto spent activated clay, Sep. Purif. Technol. 54 (2) (2007) 187–197.
[35] S.K. Ouki, M. Kavannagh, Performance of natural zeolites for the treatment of mixed metal-contaminated effluents, Waste Manage. Res. 15 (4) (1997) 383–394.
[36] E. Erdem, N. Karapinar, R. Donat, The removal of heavy metal cations by natural zeolites, J. Colloid Interf. Sci. 280 (2) (2004) 309–314.
[37] Ö. Yavuz, Y. Altunkaynak, F. Güzel, Removal of copper, nickel, cobalt and manganese from aqueous solution by kaolinite, Water Res. 37 (4) (2003) 948–952.
[38] W. Matthes, F.T. Madsen, G. Kahr, Sorption of heavy-metal cations by Al and Zr-hydroxy-intercalated and pillared bentonite, Clay Clay Miner. 47 (5) (1999) 617–629.
[39] P. Malakul, K.R. Srinivasan, H.Y. Wang, Metal adsorption and desorption characteristics of surfactant modified clay complexes, Ind. Eng. Chem. Res. 37 (11) (1998) 4296–4301.
[40] E. Alvarez-Ayuso, A. Garcia-Sanchez, Removal of heavy metals from waste waters by natural and Na-exchanged bentonites, Clay Clay Miner. 51 (5) (2003) 475–480.
[41] S.M. Hasany, M.H. Chaudhary, Sorption potential of Hare River sand for the removal of antimony from acidic aqueous solution, Appl. Radiat. Isotopes 47 (4) (1996) 467–471.
[42] F. Helfferich, Ion Exchange, McGraw-Hill, New York, 1962.
[43] Y. Yu, Y.-Y. Zhuang, Z.-H. Wang, Adsorption of water-soluble dye onto functionalized resin, J. Colloid Interf. Sci. 242 (2) (2001) 288–293.
[44] S. Lagergren, Zur theorie der sogenannten adsorption gelöster stoffe, Kungliga Svenska Vetenskapsakademiens, Handlingar 24 (4) (1898) 1–39.
[45] Y.S. Ho, G. McKay, Kinetic models for the sorption of dye from aqueous solution by wood, J. Environ. Sci. Health B: Process Safety Environ. Protect. 76 (B2) (1998) 183–191.
[46] M.J.D. Low, Kinetics of chemisorption of gases on solids, Chem. Rev. 60 (1960) 267–312.
[47] S.H. Chien, W.R. Clayton, Application of Elovich equation to the kinetics of phosphate release and sorption in soils, Soil Sci. Soc. Am. J. 44 (1980) 265–268.
[48] D.L. Sparks, Kinetics and mechanisms of chemical reactions at the soil mineral/water interface, in: D.L. Sparks (Ed.), Soil Physical Chemistry, CRC Press, Boca Raton, FL, 1999, pp. 135–192.
[49] W.J. Weber Jr., J.C. Morriss, Kinetics of adsorption on carbon from solution, J. Sanit. Eng. Div. Am. Soc. Civil Eng. 89 (1963) 31–60.
[50] A. Özcan, A.S. Özcan, Adsorption of Acid Red 57 from aqueous solutions onto surfactant-modified sepiolite, J. Hazard. Mater. 125 (1–3) (2005) 252–259.
[51] A.S. Özcan, Ş. Tetik, A. Özcan, Adsorption of acid dyes from aqueous solutions onto sepiolite, Sep. Sci. Technol. 39 (2) (2004) 301–320.
[52] K.G. Bhattacharyya, A. Sharma, *Azadirachta indica* leaf powder as an effective biosorbent for dyes: A case study with aqueous Congo Red solutions, J. Environ. Manage. 71 (3) (2004) 217–229.
[53] J.P. Chen, S. Wu, K.H. Chong, Surface modification of a granular activated carbon by citric acid for enhancement of copper adsorption, Carbon 41 (10) (2003) 1979–1986.
[54] F.-C. Wu, R.-L. Tseng, R.-S. Juang, Kinetic modeling of liquid-phase adsorption of reactive dyes and metal ions on chitosan, Water Res. 35 (3) (2001) 613–618.